On the Strength of Graphene

K. Y. Volokh
Faculty of Civil and Environmental Engineering,
Technion – Israel Institute of Technology,
Haifa, 32000 Israel
e-mail: cvolokh@technion.ac.il

Failure of a single-atomic-layer graphene sheet is analyzed in plane tension under the varying biaxiality condition. The analysis is based on the combined use of continuum and molecular mechanics where the strain energy is expressed with the help of the Tersoff-Brenner atomistic potential. A critical failure surface is produced for strains in biaxial tension. It is found that the anisotropy of graphene has a pronounced effect on its strength. [DOI: 10.1115/1.4005582]

Keywords: graphene, strength, failure, Tersoff-Brenner potential, continuum mechanics

1 Introduction

Despite theoretical fears, Novoselov et al. [1] succeeded in isolating a one-atom-thick layer of graphene. This experimental finding drew attention to the study of graphene sheets in view of their potential applications in physics, material science, and engineering [2]. Interestingly, the studies of the mechanical properties of graphene are yet relatively few [3–10].

The purpose of the present work is to obtain the failure surface for graphene under biaxial tension. To do that, a continuum-atomistic approach is adopted where the strain energy of a 2D graphene sheet is defined with the help of the Tersoff-Brenner empirical potential. The multiscale approach allows for analytically considering the problem without numerical simulations. The failure surface showing the tensile strength of graphene is presented in Fig. 3. Remarkably, the anisotropy of graphene makes a sound presence in the shape of the failure surface.

2 Continuum Mechanics

Generally, a single-atomic-layer graphene sheet should be modeled by the methods of molecular mechanics. However, in the case of the homogeneous deformation that is examined in the present work, a great deal of simplification can be achieved by a combination of molecular and continuum mechanics. In this section, the major results of continuum mechanics, relevant to the subsequent considerations, are highlighted.

In continuum mechanics the atomistic or molecular structure of material is approximated by a continuously distributed set of the so-called material points or particles. The continuum material point is an abstraction that is used to designate a small (infinitesimal) representative volume of real material, including many atoms and molecules. A material point that occupies position $\mathbf{x}$ in the reference configuration moves to position $\mathbf{y}(\mathbf{x})$ in the current configuration of the continuum. The deformation in the vicinity of the material point can be completely described by the deformation gradient tensor

$$\mathbf{F} = \partial \mathbf{y}/\partial \mathbf{x} \tag{1}$$

Using the deformation gradient, it is possible to introduce a convenient deformation measure: the right Cauchy-Green tensor

$$\mathbf{C} = \mathbf{F}^T\mathbf{F} \tag{2}$$

This tensor is good to use because it is not affected by the rigid body motion.

In the case of elastic continuum the true (Cauchy) stress is related to the strain, Eq. (2), with the following constitutive equation

$$\boldsymbol{\sigma} = 2\mathbf{F}\frac{\partial \psi}{\partial \mathbf{C}}\mathbf{F}^T \tag{3}$$

where $\psi(\mathbf{C})$ is the strain energy per unit material volume in the reference configuration.

In the absence of body and inertia forces, the stress should be divergence-free, obeying the momentum balance

$$\operatorname{div}\boldsymbol{\sigma} = \mathbf{0} \tag{4}$$

The governing Eqs. (1)–(4) should be completed with boundary conditions on tractions

$$\boldsymbol{\sigma}\mathbf{n} = \bar{\mathbf{t}} \tag{5}$$

or placements

$$\mathbf{y} = \bar{\mathbf{y}} \tag{6}$$

where $\mathbf{n}$ is the unit outward normal to the surface of the continuum and the barred quantities are prescribed.

Let us be more specific about the problem of interest in the present work and consider a biaxial tension of a thin material sheet. Since the sheet is made of a single atomic layer and the out-of-plane strains and stresses might be difficult to interpret, we restrict the considerations to the in-plane 2D continuum mechanics.

We define the Cartesian axes in the plane of the sheet as the axes of symmetry during deformation; see Fig. 1. The deformation law takes the form

$$y_1 = \lambda_1 x_1, \quad y_2 = \lambda_2 x_2 \tag{7}$$

and

$$\mathbf{F} = \lambda_1 \mathbf{e}_1 \otimes \mathbf{e}_1 + \lambda_2 \mathbf{e}_2 \otimes \mathbf{e}_2, \quad \mathbf{C} = \lambda_1^2 \mathbf{e}_1 \otimes \mathbf{e}_1 + \lambda_2^2 \mathbf{e}_2 \otimes \mathbf{e}_2 \tag{8}$$

where $\mathbf{e}_1$ and $\mathbf{e}_2$ are the Cartesian base vectors.

In view of Eq. (8) the constitutive Eq. (3) can be simplified as follows

$$\sigma_{11} = \lambda_1 \frac{\partial \psi}{\partial \lambda_1}, \quad \sigma_{22} = \lambda_2 \frac{\partial \psi}{\partial \lambda_2} \tag{9}$$

The biaxial deformation is homogeneous and, consequently, the stresses defined by Eq. (9) identically obey the momentum balance, Eq. (4). Moreover, because of the homogeneous deformation, the global elastic energy accumulated by the sheet is equal to the local strain energy times the sheet area. Assuming, in addition, that the external tensile forces (equal to σ_{11}, σ_{22}) applied at the edges of the sheet are 'dead', i.e., constant during deformation, we may formulate the criticality condition in the form

$$\begin{vmatrix} \dfrac{\partial^2 \psi}{\partial \lambda_1^2} & \dfrac{\partial^2 \psi}{\partial \lambda_1 \lambda_2} \\ \dfrac{\partial^2 \psi}{\partial \lambda_1 \lambda_2} & \dfrac{\partial^2 \psi}{\partial \lambda_2^2} \end{vmatrix} = 0 \tag{10}$$

This condition defines the singularity of the Hessian of the total potential energy, which physically means the loss of stability of

Contributed by the Applied Mechanics Division of ASME for publication in the Journal of Applied Mechanics. Manuscript received April 27, 2011; final manuscript received October 27, 2011; accepted manuscript posted February 1, 2012; published online September 13, 2012. Assoc. Editor: Yonggang Huang.

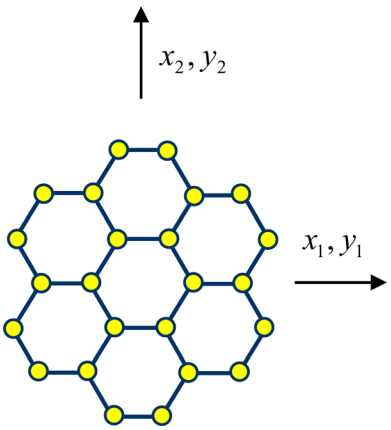

Fig. 1 Fragment of a graphene sheet

the quasi-static deformation. The loss of stability marks the onset of the material bond rupture with the subsequent failure localization and propagation. Next, we will only consider the critical point of the onset of failure without analyzing its localization and propagation.

It now remains to set the strain energy function ψ for the graphene sheet. In continuum mechanics, the latter is usually done by assuming an analytical expression for the strain energy function and fitting it to the results of macroscopic tests. At this point, however, we depart from the classical continuum mechanics and we derive the strain energy function based on the empirical atomistic potentials.

3 Molecular Mechanics

In order to derive the strain energy function from the atomistic potentials we note that the relative positions of two atoms in the referential configuration

$$\mathbf{R}_{ij} = \mathbf{R}_j - \mathbf{R}_i \tag{11}$$

can be mapped into the relative position of the same atoms in the current configuration

$$\mathbf{r}_{ij} = \mathbf{r}_j - \mathbf{r}_i \tag{12}$$

with the help of the deformation gradient

$$\mathbf{r}_{ij} = \mathbf{F}\mathbf{R}_{ij} \tag{13}$$

where $\mathbf{R}_i$ and $\mathbf{r}_i$ are the referential and current positions of the ith atom.

Equation (13) allows the linking of the atomistic and continuum descriptions. This link is tacitly assumed in the classical continuum mechanics where the infinitesimal representative material volumes locally deform in the homogeneous mode.

In crystal elasticity [11], the multiscale link, Eq. (13), is often referred to as the Cauchy-Born rule [12–14]. It is usually assumed that the Cauchy-Born rule is applicable to every simple Bravais lattice while various lattices can move independently with respect to each other. Thus, additional relaxation parameters are introduced in the theory. We do not follow this path, however, assuming that the highly symmetric deformation considered in the present work would not be essentially affected by any possible atomic relaxation. The reader can find the discussions of the applicability of the Cauchy-Born rule in Refs. [15–18], for example.

Having Eq. (13) at hand, we can express all distances and angles between the current positions of the atoms through the right Cauchy-Green tensor as follows

$$r_{ij} = \sqrt{\mathbf{r}_{ij}\cdot\mathbf{r}_{ij}} = \sqrt{\mathbf{R}_{ij}\cdot\mathbf{C}\mathbf{R}_{ij}} \tag{14}$$

$$\cos\varphi_{ijk} = \frac{\mathbf{r}_{ij}\cdot\mathbf{r}_{ik}}{r_{ij}r_{ik}} = \frac{\mathbf{R}_{ij}\cdot\mathbf{C}\mathbf{R}_{ik}}{r_{ij}r_{ik}} \tag{15}$$

Now, gathering all atomistic potentials U taking into account Eqs. (14) and (15), it is possible to set the strain energy function per unit surface area in the form

$$\psi(\mathbf{C}) = \frac{1}{2A_0}\sum_{i,j} U(r_{ij}(\mathbf{C})), \tag{16}$$

where A_0 is the area of the graphene sheet in the reference configuration.

We specify the potential for carbon following [19,20]

$$U(r_{ij}) = \frac{D}{S-1}f_c(r_{ij})\{\exp[-\sqrt{2S}\beta(r_{ij}-R_{ij})] - \frac{S}{2}(B_{ij}+B_{ji})\exp[-\sqrt{2/S}\beta(r_{ij}-R_{ij})]\} \tag{17}$$

$$R_{ij} = \sqrt{\mathbf{R}_{ij}\cdot\mathbf{R}_{ij}} \tag{18}$$

$$B_{ij} = \left\{1 + \sum_{k(\neq i,j)} a_0\left(1 + \frac{c_0^2}{d_0^2} - \frac{c_0^2}{d_0^2 + (1+\cos\varphi_{ijk})^2}\right)f_c(r_{ik})\right\}^{-\delta} \tag{19}$$

where $a_0 = 0.00020813$, $c_0 = 330$, $d_0 = 3.5$, $\delta = 0.5$, $D = 6.0$ eV, $S = 1.22$, $\beta = 21$ nm^{-1}, and $R_{ij} = 0.142$ nm is the equilibrium bond length for atoms i and j under the condition of multiatomic coupling.

The cutoff function $f_c(r_{ij})$ used in Eq. (17) is

$$f_c(r_{ij}) = \begin{cases} 1 & 0 < r_{ij} < a_1 \\ \frac{1}{2} + \frac{1}{2}\cos\frac{\pi(r_{ij}-a_1)}{a_2-a_1} & a_1 \le r_{ij} < a_2 \\ 0 & r_{ij} \ge a_2 \end{cases} \tag{20}$$

where $a_1 = 0.17$ nm and $a_2 = 0.20$ nm include the only the first-neighbor shell for carbon.

The cutoff function can be rewritten in a more compact form as follows

$$f_c(r_{ij}) = H(r_{ij}) - H(r_{ij}-a_1) + \frac{1}{2}\left\{1 + \cos\frac{\pi(r_{ij}-a_1)}{a_2-a_1}\right\} \times \{H(r_{ij}-a_1) - H(r_{ij}-a_2)\} \tag{21}$$

where the Heaviside unit step function has been used

$$H(z) = \begin{cases} 1, & z \ge 0 \\ 0, & z < 0 \end{cases} \tag{22}$$

Other potentials, accounting for two- and three-body interactions, can also be found in the literature with various cutoff functions.

4 Specialization

In this section we specialize formulas in view of the homogeneous deformation of interest. It is possible to restrict attention to the graphene pattern shadowed in Fig. 2.

In this case, the strain energy function can be written as follows

$$A_0\psi = U(r_{12}) + U(r_{13}) + U(r_{14}) \tag{23}$$

where $A_0 = 3\sqrt{3}R^2/2$ is the area of the shadowed pattern.

We calculate the first term on the right hand side of Eq. (23) as follows

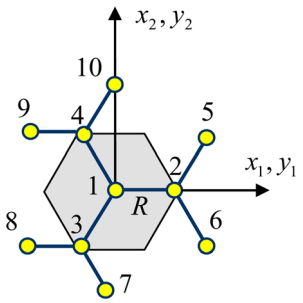

Fig. 2 Graphene pattern is shadowed in gray

$$U(r_{12}) = \frac{D}{S-1} f_c(r_{12}) \{ \exp[-\sqrt{2S}\beta(r_{12} - R)] - \frac{S}{2}(B_{12} + B_{21}) \times \exp[-\sqrt{2/S}\beta(r_{12} - R)] \} \tag{24}$$

where

$$B_{12} = \left\{ 1 + \sum_{k=3,4} a_0 \left(1 + \frac{c_0^2}{d_0^2} - \frac{c_0^2}{d_0^2 + (1 + \cos\varphi_{12k})^2} \right) f_c(r_{1k}) \right\}^{-\delta} \tag{25}$$

$$B_{21} = \left\{ 1 + \sum_{k=5,6} a_0 \left(1 + \frac{c_0^2}{d_0^2} - \frac{c_0^2}{d_0^2 + (1 + \cos\varphi_{21k})^2} \right) f_c(r_{2k}) \right\}^{-\delta} \tag{26}$$

To calculate Eqs. (24)–(28), we define the reference relative atomic positions as follows

$$\begin{cases} \mathbf{R}_{12} = R\mathbf{e}_1 \\ \mathbf{R}_{13} = -R(\mathbf{e}_1 + \sqrt{3}\mathbf{e}_2)/2 \\ \mathbf{R}_{14} = -R(\mathbf{e}_1 - \sqrt{3}\mathbf{e}_2)/2 \\ \mathbf{R}_{21} = -\mathbf{R}_{12} \\ \mathbf{R}_{25} = -\mathbf{R}_{13} \\ \mathbf{R}_{26} = -\mathbf{R}_{14} \end{cases} \tag{27}$$

Substituting Eq. (27) in Eq. (13), taking into account Eq. $(8)_1$ we obtain

$$\begin{cases} \mathbf{r}_{12} = \lambda_1 R\mathbf{e}_1 \\ \mathbf{r}_{13} = -R(\lambda_1\mathbf{e}_1 + \sqrt{3}\lambda_2\mathbf{e}_2)/2 \\ \mathbf{r}_{14} = -R(\lambda_1\mathbf{e}_1 - \sqrt{3}\lambda_2\mathbf{e}_2)/2 \\ \mathbf{r}_{21} = -\mathbf{r}_{12} \\ \mathbf{r}_{25} = -\mathbf{r}_{13} \\ \mathbf{r}_{26} = -\mathbf{r}_{14} \end{cases} \tag{28}$$

Substituting Eq. (28) in Eqs. (14) and (15) we have

$$r_{12} = \lambda_1 R, \quad r_{13} = r_{14} = r_{25} = r_{26} = \frac{R}{2}\sqrt{\lambda_1^2 + 3\lambda_2^2} \tag{29}$$

$$\cos\varphi_{123} = \cos\varphi_{124} = \cos\varphi_{215} = \cos\varphi_{216} = \frac{-\lambda_1}{\sqrt{\lambda_1^2 + 3\lambda_2^2}} \tag{30}$$

Substituting Eqs. (29) and (30) in Eqs. (25) and (26) we observe that

$$B_{12} = B_{21} \tag{31}$$

Analogously, we calculate the second term on the right hand side of Eq. (23)

$$U(r_{13}) = \frac{D}{S-1} f_c(r_{13}) \left\{ \exp[-\sqrt{2S}\beta(r_{13} - R)] - \frac{S}{2}(B_{13} + B_{31}) \times \exp[-\sqrt{2/S}\beta(r_{13} - R)] \right\} \tag{32}$$

where

$$B_{13} = \left\{ 1 + \sum_{k=2,4} a_0 \left(1 + \frac{c_0^2}{d_0^2} - \frac{c_0^2}{d_0^2 + (1 + \cos\varphi_{13k})^2} \right) f_c(r_{1k}) \right\}^{-\delta} \tag{33}$$

$$B_{31} = \left\{ 1 + \sum_{k=7,8} a_0 \left(1 + \frac{c_0^2}{d_0^2} - \frac{c_0^2}{d_0^2 + (1 + \cos\varphi_{31k})^2} \right) f_c(r_{3k}) \right\}^{-\delta} \tag{34}$$

To calculate Eqs. (32)–(34) we have Eq. $(28)_{1\text{-}3}$ and we define the lacking reference relative atomic positions as follows

$$\begin{cases} \mathbf{R}_{31} = -\mathbf{R}_{13} \\ \mathbf{R}_{37} = -\mathbf{R}_{14} \\ \mathbf{R}_{38} = -\mathbf{R}_{12} \end{cases} \tag{35}$$

Substituting Eq. (35) in Eq. (13) we obtain

$$\begin{cases} \mathbf{r}_{31} = -\mathbf{r}_{13} \\ \mathbf{r}_{37} = -\mathbf{r}_{14} \\ \mathbf{r}_{38} = -\mathbf{r}_{12} \end{cases} \tag{36}$$

Substituting Eq. $(28)_{1\text{-}3}$ and Eq. (36) in Eqs. (14) and (15) we have

$$r_{13} = r_{14} = r_{37} = \frac{R}{2}\sqrt{\lambda_1^2 + 3\lambda_2^2}, \quad r_{12} = r_{38} = \lambda_1 R \tag{37}$$

$$\cos\varphi_{132} = \cos\varphi_{318} = \frac{-\lambda_1}{\sqrt{\lambda_1^2 + 3\lambda_2^2}}, \quad \cos\varphi_{134} = \cos\varphi_{317} = \frac{\lambda_1^2 - 3\lambda_2^2}{\lambda_1^2 + 3\lambda_2^2} \tag{38}$$

Substituting Eqs. (37) and (38) in Eqs. (33) and (34) we observe that

$$B_{13} = B_{31} \tag{39}$$

Finally, we calculate the third term on the right hand side of Eq. (23)

$$U(r_{14}) = \frac{D}{S-1} f_c(r_{14}) \left\{ \exp[-\sqrt{2S}\beta(r_{14} - R)] - \frac{S}{2}(B_{14} + B_{41}) \times \exp[-\sqrt{2/S}\beta(r_{14} - R)] \right\} \tag{40}$$

where

$$B_{14} = \left\{ 1 + \sum_{k=2,3} a_0 \left(1 + \frac{c_0^2}{d_0^2} - \frac{c_0^2}{d_0^2 + (1 + \cos\varphi_{14k})^2} \right) f_c(r_{1k}) \right\}^{-\delta} \tag{41}$$

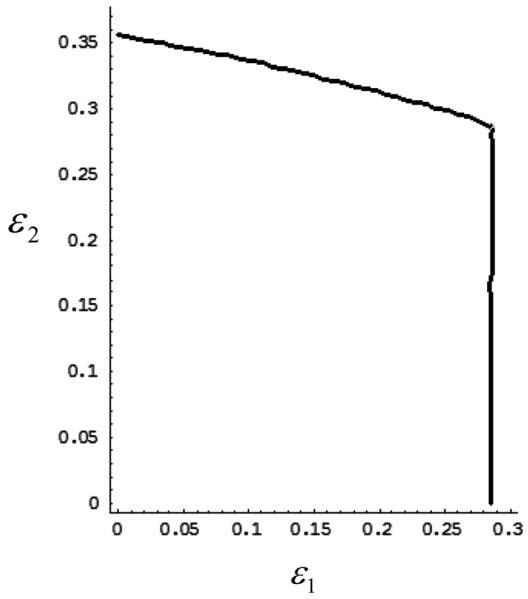

Fig. 3 Critical failure strains in biaxial tension

$$B_{41}=\left\{1+\sum_{k=9,10}a_0\left(1+\frac{c_0^2}{d_0^2}-\frac{c_0^2}{d_0^2+(1+\cos\varphi_{41k})^2}\right)f_c(r_{4k})\right\}^{-\delta} \tag{42}$$

To calculate Eqs. (41) and (42), we have Eq. $(28)_{1\text{-}3}$ and we define the lacking reference relative atomic positions as follows

$$\begin{cases}\mathbf{R}_{41}=-\mathbf{R}_{14}\\ \mathbf{R}_{410}=-\mathbf{R}_{13}\\ \mathbf{R}_{49}=-\mathbf{R}_{12}\end{cases} \tag{43}$$

Substituting Eq. (43) in Eq. (13) we get

$$\begin{cases}\mathbf{r}_{41}=-\mathbf{r}_{14}\\ \mathbf{r}_{410}=-\mathbf{r}_{13}\\ \mathbf{r}_{49}=-\mathbf{r}_{12}\end{cases} \tag{44}$$

Substituting Eq. $(28)_{1\text{-}3}$ and Eq. (44) in Eqs. (14) and (15) we have

$$r_{13}=r_{14}=r_{410}=\frac{R}{2}\sqrt{\lambda_1^2+3\lambda_2^2},\quad r_{12}=r_{49}=\lambda_1 R \tag{45}$$

$$\cos\varphi_{142}=\cos\varphi_{419}=\frac{-\lambda_1}{\sqrt{\lambda_1^2+3\lambda_2^2}},$$
$$\cos\varphi_{143}=\cos\varphi_{4110}=\frac{\lambda_1^2-3\lambda_2^2}{\lambda_1^2+3\lambda_2^2} \tag{46}$$

Substituting Eqs. (45) and (46) in Eqs. (41) and (42) we observe that

$$B_{14}=B_{41} \tag{47}$$

Thus, we have completely defined the strain energy.

5 Results and Conclusions

Based on the previously developed strain energy function and the critical instability condition in Eq. (10), it is possible to derive the critical failure surface in the 2D space defined by the engineering strains

$$\varepsilon_1=\lambda_1-1,\quad \varepsilon_2=\lambda_2-1 \tag{48}$$

This failure surface is presented in Fig. 3 for tensile strains. In the case of compressive strains, the situation is subtler because the out-of-plane buckling can occur. The latter possibility is not analyzed in the present work, which is restricted to purely tensile strains. It should also be mentioned that we do not calculate stresses because of the following two reasons. First, the very concept of stress in molecular mechanics is controversial; see [21] for a discussion. Second, even in the case of the agreement on the definition of stress, it is impossible to directly measure it in contrast to strain that can be measured in experiments.

It is remarkable that the critical failure surface shows a pronounced anisotropy of the graphene strength. Indeed, the tensile strength in direction x_1 does not depend on the strain in direction x_2. The latter independence occurs because the horizontal bonds control failure in direction x_1 and they are not affected by the deformation in the perpendicular direction; see Fig. 1. At the same time, there are no bonds aligned with direction x_2 and the tensile strength in direction x_2 is controlled by the inclined bonds that are affected by the deformation in direction x_1. The latter effect is presented on the top of the failure surface in Fig. 3; the critical strain in the uniaxial tension is greater than in the equal-biaxial one. The latter difference is explained by the fact that the strain energy, which is limited, is consumed by straining in one direction only in the case of the uniaxial tension $\varepsilon_1=0$; while the same amount of energy is consumed by straining in two directions simultaneously in the case of equal biaxial tension $\varepsilon_1=\varepsilon_2$.

We note, finally, that the graphene sheet was assumed to be ideal without defects, which might trigger a much earlier onset of failure than predicted in Fig. 3. Besides, temperature effects might also affect failure [22].

References

[1] Novoselov, K. S., Jiang, D., Schedin, F., Booth, T. J., Khotkevich, V. V., Morozov, S. V., and Geim, A. K., 2005, "Two-Dimensional Atomic Crystals," Proc. Natl. Acad. Sci. U.S.A., **102**, pp. 10451–10453.

[2] Geim, A. K. and Novoselov, K. S., 2007, "The Rise of Graphene," Nature Mater., **6**, pp. 183–191.

[3] Khare, R., Mielke, S. L., Paci, J. T., Zhang, S. L., Ballarini, R., Schatz, G. C., and Belytschko, T., 2007, "Coupled Quantum Mechanical/Molecular Mechanical Modeling of the Fracture of Defective Carbon Nanotubes and Graphene Sheets," Phys. Rev. B, **75**, p. 075412.

[4] Liu, F., Ming, P. M., and Li, J., 2007, "Ab Initio Calculation of Ideal Strength and Phonon Instability of Graphene Under Tension," Phys. Rev. B, **76**, p. 064120.

[5] Reddy, C. D., Rajendran, S., and Liew, K. M., 2006, "Equilibrium Configuration and Continuum Elastic Properties of Finite Sized Graphene," Nanotechnology, **17**, pp. 864–870.

[6] Zhou, J. and Huang, R., 2008, "Internal Lattice Relaxation of Single-Layer Graphene Under In-Plane Deformation," J. Mech. Phys. Solids, **56**, pp. 1609–1623.

[7] Lu, Q. and Huang, R., 2009, "Nonlinear Mechanics of Single-Atomic-Layer Graphene Sheets," Int. J. Appl. Mech., **3**, pp. 443–467.

[8] Lee, C., Wei, X., Kysar, J. W., and Hone, J., 2008, "Measurement of the Elastic Properties and Intrinsic Strength of Monolayer Graphene," Science, **321**, pp. 385–388.

[9] Wei, X., Fragneaud, B., Marianetti, C. A., and Kysar, J. W., 2009, "Nonlinear Elastic Behavior of Graphene: Ab Initio Calculations to Continuum Description," Phys. Rev. B, **80**, p. 205407.

[10] Marianetti, C. A. and Yevick, H. G., 2010, "Failure Mechanisms of Graphene Under Tension," Phys. Rev. Lett., **105**, p. 245502.

[11] Beatty, M. F. and Hayes, M. A., 2005, *Mechanics and Mathematics of Crystals. Selected Papers of J. L. Ericksen*, World Scientific, Singapore.

[12] Born, M. and Huang, K., 1954, *Dynamical Theory of the Crystal Lattices*, Oxford University Press, Oxford.

[13] Weiner, J. H., 1983, *Statistical Mechanics of Elasticity*, Wiley, New York.

[14] Tadmor, E. B., Ortiz, M., and Phillips, R., 1996, "Quasicontinuum Analysis of Defects in Solids," Philos. Mag. A, **73**, pp. 1529–1563.

[15] Arroyo, M. and Belytschko, T., 2004, "Finite Crystal Elasticity of Carbon Nanotubes Based on the Exponential Cauchy-Born Rule," Phys. Rev. B, **69**, p. 115415.
[16] Huang, Y., Wu, J., and Hwang, K. C., 2006, "Thickness of Graphene and Single-Wall Carbon Nanotubes," Phys. Rev. B, **74**, p. 245413.
[17] Zhang, P., Jiang, H., Huang, Y., Geubelle, P. H., and Hwang, K. C., 2004, "An Atomistic-Based Continuum Theory for Carbon Nanotubes: Analysis of Fracture Nucleation," J. Mech. Phys. Solids, **52**, pp. 977–998.
[18] Wu, J., Hwang, K. C., and Huang, Y., 2008, "An Atomistic-Based Finite-Deformation Shell Theory for Single-Wall Carbon Nanotubes," J. Mech. Phys. Solids, **56**, pp. 279–292.
[19] Tersoff, J., 1988, "New Empirical Approach for the Structure and Energy of Covalent Systems," Phys. Rev. B, **37**, pp. 6991–7000.
[20] Brenner, D. W., 1990, "Empirical Potential for Hydrocarbons for Use in Simulating the Chemical Vapor Deposition of Diamond Films," Phys. Rev. B, **42**, pp. 9458–9471.
[21] Admal, N. C. and Tadmor, E. B., 2010, "A Unified Interpretation of Stress in Molecular Systems," J. Elasticity, **100**, pp. 63–143.
[22] Zhao, H. and Aluru, N. R., 2010, "Temperature and Strain-Rate Dependent Fracture Strength of Graphene," J. Appl. Phys., **108**, p. 064321.